Journal of Photochemistry and Photobiology A: Chemistry 199 (2008) 224–229

Contents lists available at ScienceDirect

Journal of Photochemistry and Photobiology A: Chemistry

journal homepage: www.elsevier.com/locate/jphotochem

Effects of electron donors on the performance of plasmon-induced photovoltaic cell

Yang Tian [a,*], Xiting Wang [a], Da Zhang [a], Xiu Shi [a], Shilong Wang [b]

[a] Department of Chemistry, Tongji University, Siping Road 1239, Shanghai 200092, PR China
[b] School of Life Science and Technology, Tongji University, Siping Road 1239, Shanghai 200092, PR China

ARTICLE INFO

Article history:
Received 9 December 2007
Received in revised form 26 March 2008
Accepted 30 May 2008
Available online 21 June 2008

Keywords:
Charge separation
Plasmon
Photovoltaic cell
Electron donor
Transient absorption spectroscopy

ABSTRACT

In this paper, charge separation of Au–TiO_2 nanocomposites under visible light irradiation is investigated by transient absorption spectroscopy (TAS), as well as steady-state absorbance studies. The effects of electron donors on the performance of plasmon-induced photovoltaic cell are studied by employing three kinds of donors: $[Fe(CN)_6]^{4-}$, Fe^{2+}, and ferrocenecarboxylic acid, since the apparent formal potential of $[Fe(CN)_6]^{4-}$ and ferrocenecarboxylic acid is more negative and more positive than that of Fe^{2+}, respectively, providing the opportunity to determine the influence of donors on the open-circuit photovoltage and short-circuit photocurrent. The experimental results indicate that both the open-circuit photovoltage and the short-circuit photocurrent are not simply dependent on the apparent formal potential of the donors. In addition, transient absorbance measurements show that the regeneration rates of the oxidized gold nanoparticles decreases in the order: Fe^{2+} > ferrocenecarboxylic acid > $[Fe(CN)_6]^{4-}$.

1. Introduction

Recently, noble metal nanoparticles, such as gold and silver, have been attracting more and more research attentions, because of their unique physical and chemical properties different from bulk metals and the potential applications, such as electronic, optical, thermal, catalytic, and magnetic devices [1–8]. Surface plasmon resonance is just one of the most striking characteristics of gold and silver in nanometer scales, and has been widely recognized in the field of surface science since the pioneering work of Ritchie [9]. The unique plasmon absorbance features of noble metal nanoparticles have been exploited for wide applications, including chemical sensors and biosensors, to produce silver nanoprisms and gold nanorods, and so on [6–8,10–18].

In the previous work [19–21], plasmon-induced photoeletrochemistry at gold and silver nanoparticles incorporated in nanoporous TiO_2 have been reported. Charge separation is realized at noble metal nanoparticles-TiO_2 nanocomposites and is currently being exploited for a wide of applications, such as photovoltaic cells, visible light-responsive photocatalysis, and surface patterning. The mechanism of charge separation is proposed as: the visible light generates the photoexcited state of the gold nanoparticles based on the surface plasmon resonance. Then the photoexcited electrons are injected into the TiO_2 bulk. Simultaneously, the oxidized gold nanoparticles take electrons from a donor in the solution. Furube et al. directly observed plasmon-induced electron transfer from 10 nm gold nanodots to TiO_2 nanoparticles by using femtosecond transient absorption spectroscopy (TAS) with an IR probe [22].

For the sake of confirming the mechanism of charge separation at Au–TiO_2 nanocomposites under visible light-irradiation, and further understanding the effects of electron donors on the performance of this plasmon-induced photovoltaic cell, subsequently achieving the total energy efficiency of the photovoltaic cell, TAS is employed in the present work. TAS is a powerful tool for probing charge separation and electron transfer, since electron transfer is always in sub-microsecond, nanosecond, even in picosecond grade. Here, transient absorbance measurements, as well as steady-state spectroscopic studies are evident of that charge separation is accomplished at mixture suspension of gold nanoparticles and TiO_2 under visible light illumination. In addition, we investigate two typical kinds of donors, $[Fe(CN)_6]^{4-}$ and ferrocenecarboxylic acid, compared to Fe^{2+} since the apparent formal potential of $[Fe(CN)_6]^{4-}$ and ferrocenecarboxylic acid is more negative and more positive than that of Fe^{2+}, respectively. The electron donor influences on the plasmon-induced photovoltaic cell performance is also determined using transient absorption spectroscopic and photoelectrochemical measurements.

* Corresponding author. Tel.: +86 21 65987075; fax: +86 21 65982287.
E-mail address: yangtian@mail.tongji.edu.cn (Y. Tian).

1010-6030/$ – see front matter © 2008 Elsevier B.V. All rights reserved.
doi:10.1016/j.jphotochem.2008.05.025

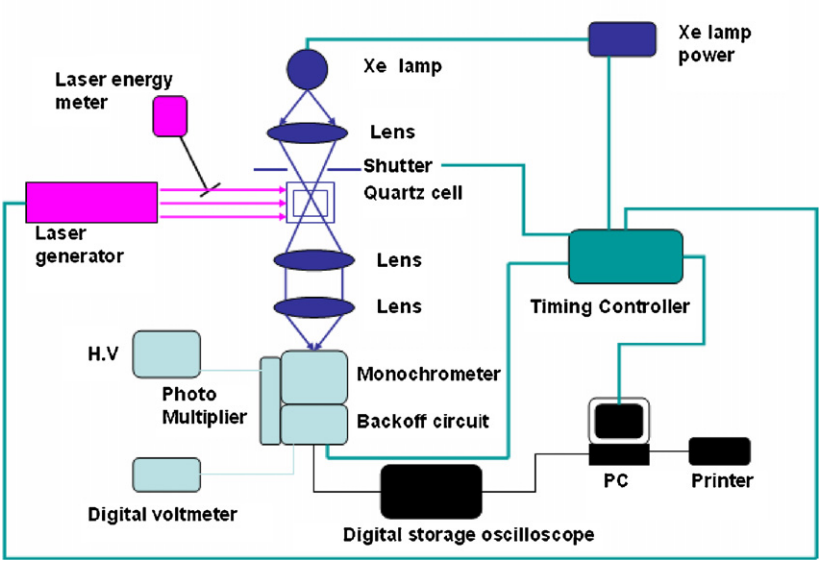

Fig. 1. Schematic diagram of the apparatus for nanosecond transient absorption spectroscopy.

2. Experimental

Acetonitrile (analytical grade), ethylene glycol (analytical grade), lithium nitrate, iron(II) chloride, potassium ferrocyanide, ethanol (99.5%), and methanol (99.5%) were purchased from Sinopharm Chemical Reagent Co., Ltd. (Shanghai, China) and used as supplied. Hydrogen tetrachloroaurate(III) ($HAuCl_4$) trihydrate and ferrocenecarboxylic acid was obtained from Aldrich Chemical Company, Inc. (USA) and used without further purification. The solution used in this work was freshly prepared and deoxygenated for bubbling nitrogen gas for at least 30 min prior to use.

A TiO_2 film was prepared as follows: an ITO-coated glass plate was coated with a nanoporous TiO_2 film prepared from an anatase TiO_2 sol (Ishihara Sangyo Kaisha, STS-21, 20 nm particle diameter) by spin-coating (sintered at 723 K for 1 h). For the preparation of a Au–TiO_2 film: a TiO_2 film was soaked in a 5 mM aqueous $HAuCl_4$ for about 30 min and rinsed with water. Then, the film was irradiated with ultraviolet light (1 mW cm^{-2}) for at least 1 h to reduce the adsorbed Au^{3+} to Au by TiO_2 photocatalysis at the expense of water oxidation. Gold nanoparticles suspended in solution was prepared by the method previously reported [23]. The substrate was immersed in the suspension for 12–15 h and was rinsed thoroughly with ethanol.

A CHI 660 electrochemical work station (CH instruments, USA) was employed in all electrochemical measurements. To test the performance of each electron donor, a platinum wire was employed as the counter electrode in a two-compartment two-electrode cell. On the other hand, open-circuit photovoltage, short-circuit photocurrent, the total energy conversion efficiency were obtained in a two-electrode sandwich cell (thickness of the electrolyte, 5 mm). The counter electrode was a platinum plate. The Au–TiO_2 substrate was irradiated with a white light ($\lambda > 420$ nm) using a xenon lamp with an ultraviolet-cut filter from the back.

The steady-state UV absorption spectra were measured using an Agilent 8453 UV–vis–NIR spectrophotometer (Agilent Instruments, USA). Transient absorbance spectroscopic measurements were performed as shown in Fig. 1. A pulse of approximately 6 ns at 532 nm from a Nd:YAG Q-switched laser was used as the excitation source. A white light source was the probe beam (300 W Xe) and was positioned normal to the excitation beam.

3. Results and discussion

Fig. 2 shows the TEM images of (A) TiO_2 and (B) gold colloids employed in the present work. The commercial TiO_2 and the prepared gold colloids are suspended into the solutions very well, and are in the diameter of 20–50 nm and 20–30 nm, respectively. The plasmon resonance absorption peak of gold nanoparticles is located near 535 nm, as depicted in curve a of Fig. 3(A).

Fig. 3(A) shows UV–vis spectra of (a) gold nanoparticles, (b–d) the mixture suspension of TiO_2 and gold nanoparticles following the visible white light irradiation; Fig. 3(B) demonstrates the changes in the absorption spectra following the illumination of visible light at the mixture suspension of TiO_2 and gold nanoparticles in the deaerated solution. Before subjecting to white light-irradiation, the plasmon absorption peak of gold nanoparticles is observed at 535 nm (Fig. 3(A)a). As gold nanoparticles were irradiated under white light for 10 min with the addition of TiO_2 colloids, the plasmon absorption peak of gold nanoparticles located at around 535 nm decreased with the increasing broad absorption of 600–800 nm (Fig. 3(A)b and (B)a). After the mixture suspension of TiO_2 and gold nanoparticles were irradiated with visible white light for ~20 min (Fig. 3(A)c and (B)b), and for ~30 min (Fig. 3(A)d and (B)c), the absorption peak at around 535 nm continuously decreased, combined with the consecutive increase of the broad absorption peak from 600 to 800 nm. It is well-known that the TiO_2 colloids exhibit broad absorption in the 400–800 nm regions, corresponding to the trapping of electrons at Ti^{4+} sites. The Ti^{3+} centers formed as a result of electron trapping have been characteristic in earlier studies [24–27]. The mixture suspension of TiO_2 and gold nanoparticles shows strong bleaching in the plasmon absorption region in addition to the absorption in the red. The control experiments in the absence of TiO_2 were also carried out. Fig. 3(C) depicts UV–vis spectra of gold nanoparticles solution after irradiated by white light for 0 min (a), 10 min (b), 20 min (c), and 30 min (d). Fig. 3(D) demonstrates the changes in the absorption spectra of gold nanoparticles following the illumination of white light in the absence of TiO_2 colloid. The absorption peaks of gold nanoparticles at around 535 nm had a little decrease following the irradiation of white light, compared with Fig. 3(A) and (B), and without obvious increase of the broad absorption peak from 600 to 800 nm, corresponding to the trapping of electrons at Ti^{4+} sites.

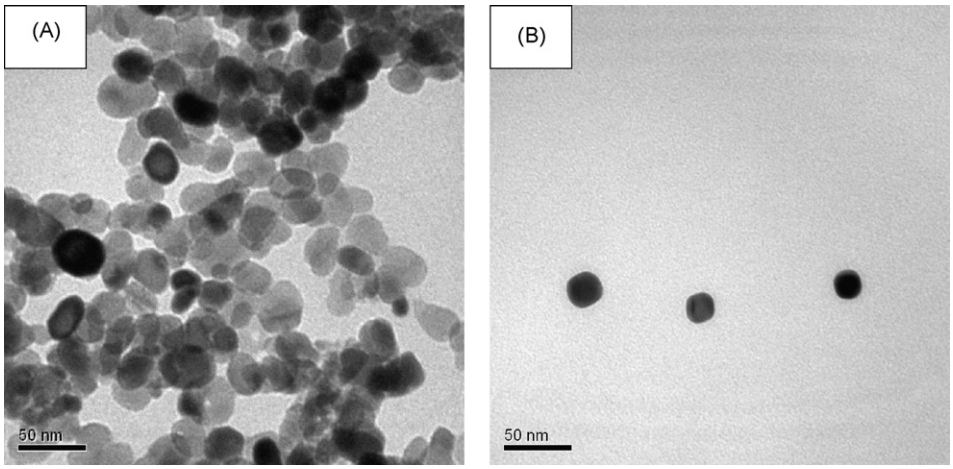

Fig. 2. Transmission electron micrographs (TEMs) of (A) TiO_2 and (B) gold colloids.

It demonstrated that gold nanoparticles are excited under visible light irradiation and undergo charge separation due to the surface plasmon resonance, even in the absence of TiO_2. However, recombination of electron transfer may be very rapidly, and as a result the changes in spectra of gold nanoparticles under white light irradiation were very small, suggesting that TiO_2 is essential for the spectra changes, and the photogenerated electrons are transferred to TiO_2 conduction band. This conclusion is also confirmed by transient absorption spectroscopy, as demonstrated later.

Fig. 4(A) depicts the time evolution of the transient absorption spectra observed in TiO_2 and gold nanocomposites suspended in the deaerated solution. A negative feature is observed around 530 nm, which is ascribed to the bleaching of gold nanoparticles absorption upon electronic excitation resulted from surface plasmon resonance and electron injection into the TiO_2 conduction band. Meanwhile, a positive broad peak is obtained in the red region due to the electron storage in TiO_2 particles produced by the charge injection process. In the absence of redox couples, the only mech-

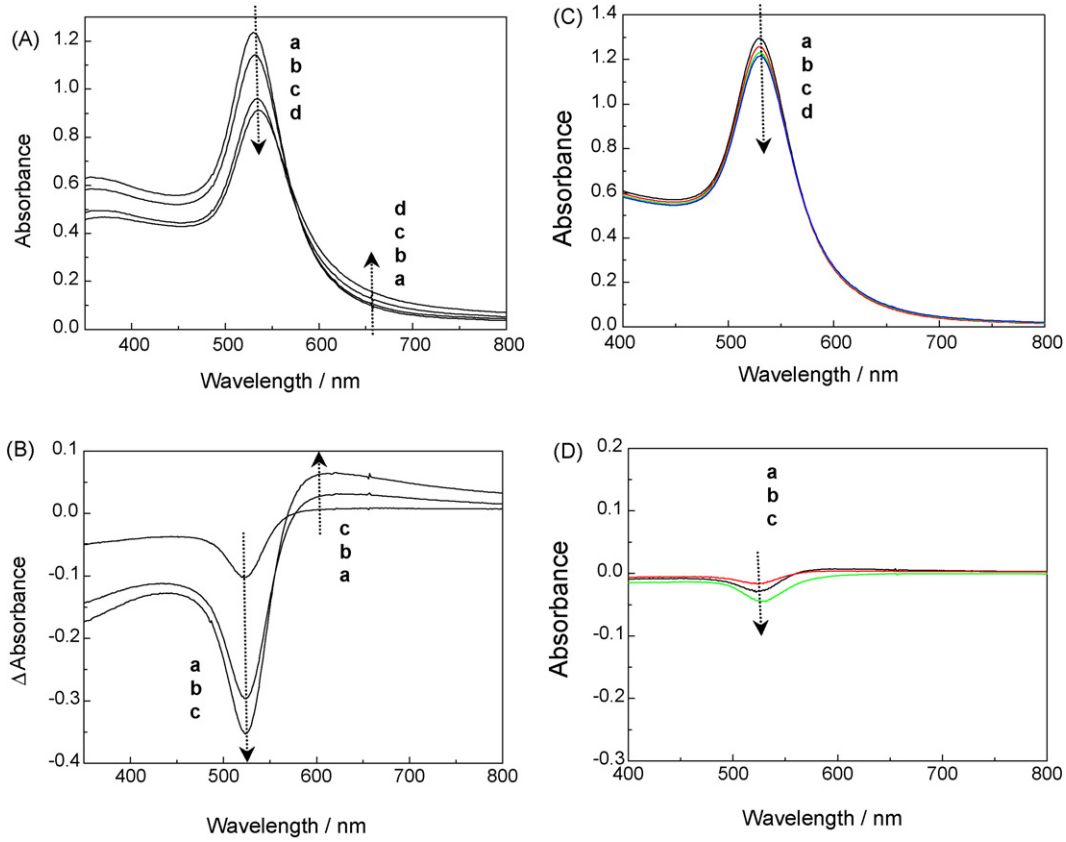

Fig. 3. (A) UV–vis absorption spectra of (a) gold nanoparticles, (b) gold nanoparticles after 10 min white light-irradiation with the addition of TiO_2 colloids, (c) after irradiated for ~20 min, and (d) after irradiated for ~30 min. (B) UV–vis absorption spectra changes of (a) gold nanoparticles after 10 min visible light-irradiation with the addition of TiO_2 colloids, (b) Au–TiO_2 nanocomposites irradiated for ~20 min, and (c) Au–TiO_2 nanocomposites irradiated for ~30 min. Data were obtained from (A). (C) UV–vis absorption spectra of (a) gold nanoparticles, (b) gold nanoparticles after 10 min white light-irradiation, (c) after irradiated for ~20 min, and (d) after irradiated for ~30 min. (D) UV–vis absorption spectra changes of (a) gold nanoparticles after 10 min white light-irradiation, (b) after irradiated for ~20 min, and (c) after irradiated for ~30 min. All experiments were carried out in a deaerated solution.

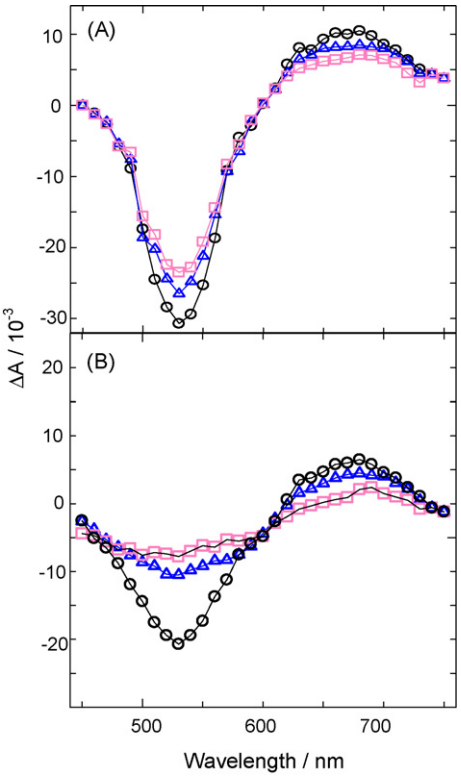

Fig. 4. Transient absorption spectra obtained upon nanosecond pulsed laser excitation of gold nanoparticles in TiO_2 suspended solution in the absence (A) and in the presence (B) of redox couple Fe^{2+}. Absorbance changes are recorded 50 (–○–), 200 (–△–), and 500 (–□–) ns after the laser excitation (λ = 532 nm, 5 ns pulse duration) was applied. The experiments were carried out in a deaerated solution.

anism for gold nanoparticles regeneration is back electron transfer from the conduction band of TiO_2 to the oxidized gold nanoparticles. From Fig. 4(A), we can see that this recombination process is relatively slow, and only a minor portion of excited gold nanoparticles is recovered in the sub-microsecond time scale. On the other hand, in the presence of redox couple (Fig. 4(B)), such as Fe^{2+}/Fe^{3+}, regeneration of the gold nanoparticles absorption following charge injection is clearly faster, indicating the photoexcited gold nanoparticles due to surface plasmon resonance takes electrons rapidly from the electron transfer donor (Fe^{2+}) in the solution.

Therefore, not only steady-state photolysis data but also transient absorption studies using laser flash photolysis gave the strong evidence that charge was separated at Au–TiO_2 nanocomposites under visible light irradiation. And the mechanism of charge separation is that gold nanoparticles are photoexcited under visible light illumination due to surface plasmon resonance, and the generated electrons are injected into the TiO_2 conduction band. In the presence of redox couples, the oxidized gold nanoparticles take electrons from the donor and regenerate rapidly.

As demonstrated above, charge was completely separated at Au–TiO_2 nanocomposites under visible light illumination. This gives the strong basis for constructing the photovoltaic cell by employing gold nanoparticles as a sensitizer. As our previously reported [20], the total energy conversion efficiency of the photovoltaic cell was achieved to be about 1.27% in the presence of Fe^{2+}/Fe^{3+} redox couple. To further understand the effects of the donors on the open-circuit photovoltage and short-circuit photocurrent, consequently to improve the energy conversion efficiency of photovoltaic cell more, here we investigated the other two typical kinds of donors, $[Fe(CN)_6]^{4-}$ and ferrocenecarboxylic acid, compared to Fe^{2+} since the apparent formal potential of $[Fe(CN)_6]^{4-}$ and ferrocenecarboxylic acid is more negative and more positive than that of Fe^{2+}, respectively.

Fig. 5 shows cyclic voltammograms (CVs) for three kinds of redox couples: $[Fe(CN)_6]^{4-}/[Fe(CN)_6]^{3-}$, Fe^{2+}/Fe^{3+}, and $FcCOOH/FcCOOH^+$, obtained at platinum electrode in acetonitrile and ethylene glycol (v/v: 60/40) containing 0.1 M $LiNO_3$. Apparent formal potentials $E^{0\prime}_{app}$ of each donor was calculated as the average of anodic and cathodic peak potentials [$E^{0\prime}_{app} = (E_{p,a} + E_{p,c})/2$].

Photocurrent–voltage curves for cells with the three kinds of redox couples were monitored under the same monochromatic light intensity (Fig. 6), and the characteristics of the photovoltaic cells were also summarized in Table 1. The open-circuit voltage is highest for the ferrocenecarboxylic acid and lowest for $[Fe(CN)_6]^{4-}$, indicating that the open-circuit photovoltage increased as the apparent formal potential shifted positively. The increase is usu-

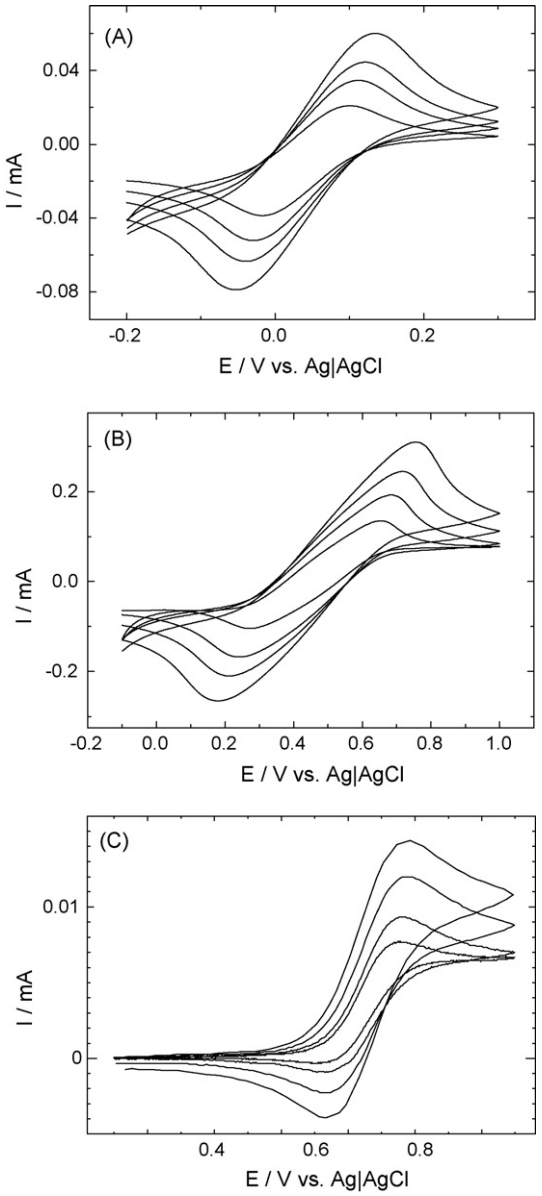

Fig. 5. Cyclic voltammograms (CVs) obtained at Pt electrode in acetonitrile and ethylene glycol (v/v: 60/40) containing 0.1 M $LiNO_3$ in the presence of 0.1 M $[Fe(CN)_6]^{4-}/[Fe(CN)_6]^{3-}$ (A), 0.1 M Fe^{2+}/Fe^{3+} (B), and 0.1 M $C_{10}H_9FeCOO^-/C_{10}H_9FeCOOH$ (C). Potential scan rates: 10, 20, 30, and 50 mV s^{-1} (from inner to outer).

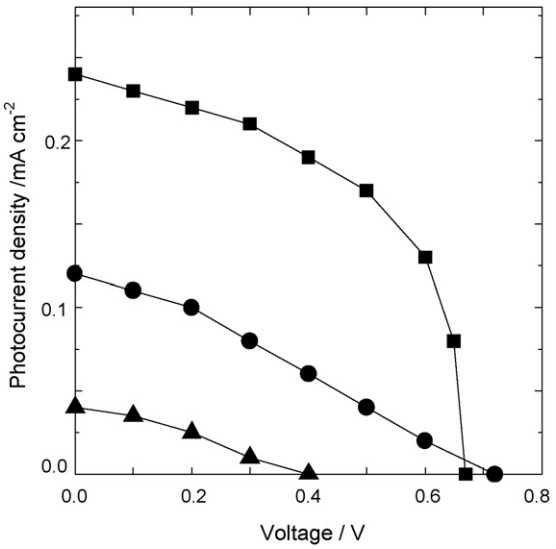

Fig. 6. Photocurrent–voltage characteristic of the cell with the Au–TiO_2 film photoanode, a Pt cathode, and the acetonitrile–ethylene glycol solution containing 0.1 M $LiNO_3$ in the presence of 0.1 M Fe^{2+} (–■–), $C_{10}H_9FeCOOH$ (–●–), and $[Fe(CN)_6]^{4-}$ (–▲–), under white light illumination (>420 nm, 10 mW cm^{-2}).

ally explained in terms of a simple positive shift in the platinum counter electrode potential with the apparent formal potential. Actually, under open-circuit condition, the potential of the Au–TiO_2 photoanodic electrode is shifted with the redox potential of donor, suggesting that the open-circuit photovoltage of the present cell is simply independent of the redox potential. As a consequence, the possible gain in V_{oc} by selecting redox couples with more positive potentials could not be realized.

On the other hand, the short-circuit current intensity increases to 0.24 mA cm^{-2} for Fe^{2+}, but only 0.12 and 0.04 mA cm^{-2} for ferrocenecarboxylic acid and $[Fe(CN)_6]^{4-}$, respectively. For probing the kinetics of gold nanoparticles regeneration by recombination of the injected electrons in TiO_2 with the oxidized gold nanoparticles or reduction by the acceptors (reducing agents) in solution, transient absorbance measurements were performed on Au–TiO_2 nanocomposites in the absence and in the presence of the three kinds of donors.

Fig. 7 shows the absorbance change after 532 nm laser pulse for Au–TiO_2 nanocomposites versus time at 530 nm in the absence (curve a) and in the presence (curve b) of $[Fe(CN)_6]^{4-}$ (Fig. 7(A)), Fe^{2+} (Fig. 7(B)), and ferrocenecarboxylic acid (Fig. 7(C)). The laser pulse generates the excited state of gold nanoparticles due to surface plasmon resonance, and then electrons are injected into the TiO_2 conduction band within 10 ns instrument response time. Therefore, the oxidized gold nanoparticles are immediately formed after the laser pulse, resulting in an obvious decrease of the absorbance at 530 nm. The magnitude of the initial absorption change is directly proportional to the quantum yield for electron injection. In the absence of an electron donor (curve a), all the injected electrons recombine with oxidized gold nanoparticles, and complete recombination requires milliseconds (data not shown). In the presence of the donor (curve b), the initial absorption changes is the intrinsic same as in the absence of the electron donor in solution, within experimental error. Following electron transfer into TiO_2, oxidized gold nanoparticles can be regenerated by the back electron in TiO_2 or competitively by the electron donor. As shown in Fig. 7(A), in the presence of $[Fe(CN)_6]^{4-}$, the regeneration of gold nanoparticles is relatively slow, and can hardly be distinguished from the transient spectrum obtained in the absence of $[Fe(CN)_6]^{4-}$. However, in the Fe^{2+} solution (Fig. 7(B)), the oxidized gold nanoparticles is rapidly regenerated within 500 ns, subsequently inhibiting significant recombination from electrons in TiO_2. This result is in a good agreement with that demonstrated in Fig. 4(B). With ferrocenecarboxylic acid (Fig. 7(C)), only a fraction of the oxidized gold nanoparticles remains about 4.5 μs after the laser pulse, suggesting that ferrocenecarboxylic acid can also regenerate the oxidized gold nanoparticles, although the regeneration rate is much slower than that in the Fe^{2+} solution. These results indicate that electron transfer from the donor to the oxidized gold nanoparticles may play a dominant role for Fe^{2+}, while that back electron transfer from the TiO_2 to the oxidized gold nanoparticles may play an important role in the presence of $[Fe(CN)_6]^{4-}$. It is obvious that there is an optimum potential for the donor/acceptor redox couple. The potential should be more negative than that of the hole on the gold nanoparticles; otherwise the gold nanoparticles cannot obtain electrons from the donor. On the other hand, the potential should be more positive than that of the TiO_2 conduction band; otherwise the acceptor cannot receive electrons from the gold nanoparticles via TiO_2 and the counter electrode. The potential of Fe^{2+}/Fe^{3+} redox couple may locate at the most proper position among that of the three kinds of redox couples, and consequently in the presence of Fe^{2+}, the oxidized gold nanoparticles obtained electrons from the donor more

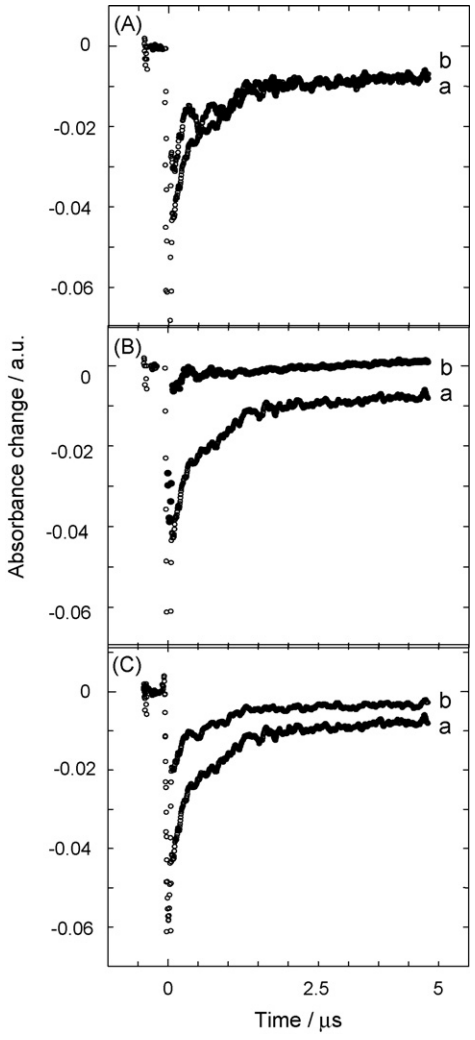

Fig. 7. Transient absorbance changes at 530 nm for the mixture suspension of TiO_2 and gold nanoparticles in acetonitrile and ethylene glycol (v/v: 60/40) containing 0.1 M $LiNO_3$ in the absence (a) and in the presence (b) of 0.1 M $[Fe(CN)_6]^{4-}$ (A), 0.1 M Fe^{2+} (B), and 0.1 M $C_{10}H_9FeCOOH$ (C).

rapidly than in the presence of the other kinds of donors. This is the key point that short-circuit current is greatest for Fe^{2+} among the three kinds of electron donors. These investigations provide a methodology to select a redox couple: only the redox couple with rapid generation ability of electron transfer from the donor to the oxidized gold nanoparticles yields the great short-circuit photocurrent, therefore generates efficient energy efficiency.

4. Conclusions

Three kinds of electron donors were evaluated for determining the effects of the formal potential of donor on the energetics and kinetics of Au-sensitized photoelectrochemical cells. The experimental data revealed that selecting a donor with more positive formal potential could not lead to an increase of the open-circuit photovoltage. Transient absorbance studies indicated that the lower short-circuit photocurrent and the efficiency were related to a slower regeneration rate of oxidized gold nanoparticles when $[Fe(CN)_6]^{4-}$ or ferrocenecarboxylic acid were used in place of Fe^{2+}. Consequently, a greater fraction of the injected electrons may recombine with the oxidized gold nanoparticles, or with electron acceptors in solution. This study provided a methodology to further understand the effects of the donors on the open-circuit photovoltage and short-circuit photocurrent, and to improve the total energy conversion efficiency of the present and the other photovoltaic cells more.

Acknowledgements

The authors thank Mr. Qianqian Yan at Tongji University for technical assistance and helpful discussions. This work was financially supported by the National Natural Science Foundation of China (20643002 for Y.T. and 30570376 for S.W.), the Program for New Century Excellent Talents in University (NCET-06-0380) and the project sponsored by the Scientific Research Foundation for the Returned Overseas Chinese Scholars from the Ministry of Education, China, and the Shanghai Pujiang Program (06PJ14090). Tongji University is also greatly acknowledged.

References

[1] C.B. Murry, C.R. Kagan, M.G. Bawendi, Science 270 (1995) 1335–1338.
[2] R.F. Ziolo, E.P. Giannelis, B.A. Weinstein, M.P. O'Horo, B.N. Ganguly, V. Mehrotra, M.W. Russell, D.R. Huffmann, Science 257 (1992) 219–223.
[3] Y.S. Kang, S. Risbud, J.F. Rabolt, P. Stroeve, Chem. Mater. 8 (1996) 2209–2211.
[4] C.P. Collier, R.J. Saykally, J.J. Shiang, S.E.H.J.R. Henrichs, Science 277 (1997) 1978–1981.
[5] M. Zhao, L. Sun, R.M. Crooks, J. Am. Chem. Soc. 120 (1998) 4877–4878.
[6] S. Link, M.A. El-Sayed, J. Phys. Chem. B 103 (1999) 8410–8426.
[7] R. Jin, Y.C. Cao, C.A. Mirkin, K.L. Kelly, G.C. Schatzand, J.G. Zheng, Science 294 (2001) 1901–1903.
[8] J.J. Mock, M. Barbic, D.R. Smith, D.A. Schults, S. Schults, J. Chem. Phys. 116 (2002) 6755–6759.
[9] R.H. Ritchie, Phys. Rev. 106 (1957) 874–881.
[10] Y. Tian, H. Liu, G. Zhao, T. Tatsuma, J. Phys. Chem. B 110 (2006) 23478–23481.
[11] Y. Tian, H. Liu, Z. Deng, Chem. Mater. 18 (2006) 5820–5822.
[12] H. Liu, Y. Tian, Z. Deng, Langmuir 23 (2007) 9487–9494.
[13] M.-C. Daniel, D. Astruc, Chem. Rev. 104 (2004) 293–346.
[14] R. Jin, Y.C. Cao, E. Hao, G.S. Métrauz, G.C. Schatz, C.A. Mirkin, Nature 425 (2003) 487–490.
[15] F. Kim, J.H. Song, P. Yang, J. Am. Chem. Soc. 124 (2002) 14316–14317.
[16] B.O. Wilson, G.J. Wilson, P. Mulvaney, Adv. Mater. 14 (2002) 1000–1004.
[17] Y. Ohko, T. Tatsuma, T. Fujii, K. Naoi, C. Niwa, Y. Kubota, A. Fujishima, Nat. Mater. 2 (2003) 29–31.
[18] K. Naoi, Y. Ohko, T. Tatsuma, J. Am. Chem. Soc. 126 (2004) 3664–3668.
[19] Y. Tian, T. Tatsuma, Chem. Commun. (2004) 1810–1811.
[20] Y. Tian, T. Tatsuma, J. Am. Chem. Soc. 127 (2005) 7632–7637.
[21] Y. Tian, H. Notsu, T. Tatsuma, Photochem. Photobiol. Sci. 4 (2005) 598–601.
[22] A. Furube, L. Du, K. Hara, R. Katoh, M. Tachiya, J. Am. Chem. Soc. 129 (2007) 14852–14853.
[23] K.R. Brown, D.G. Walter, M.J. Natan, Chem. Mater. 12 (2000) 306–313.
[24] R.F. Howe, M. Graetzel, J. Phys. Chem. 89 (1985) 4495–4499.
[25] D. Bahnemann, A. Henglein, J. Lilie, L. Spanhel, J. Phys. Chem. 88 (1984) 709–711.
[26] K.R. Gopidas, M. Bohorquez, P.V. Kamat, J. Phys. Chem. 94 (1990) 6435–6440.
[27] T. Rajh, A.E. Ostafin, O.I. Micic, D.M. Tiede, M.C. Thurnauer, J. Phys. Chem. 100 (1996) 4538–4545.